Title

Pharmacokinetics and Model-Based Dosing to Optimize Fludarabine Therapy in Pediatric Hematopoietic Cell Transplant Recipients

Journal

Transplantation and Cellular Therapy, 23(10)

ISSN

2666-6367

Authors

Ivaturi, Vijay
Dvorak, Christopher C
Chan, Danna
et al.

Publication Date

2017-10-01

DOI

10.1016/j.bbmt.2017.06.021

HHS Public Access

Author manuscript

Biol Blood Marrow Transplant. Author manuscript; available in PMC 2018 August 24.

Published in final edited form as:

Biol Blood Marrow Transplant. 2017 October ; 23(10): 1701–1713. doi:10.1016/j.bbmt.2017.06.021.

Pharmacokinetics and Model-Based Dosing to Optimize Fludarabine Therapy in Pediatric Hematopoietic Cell Transplant Recipients

Vijay Ivaturi[1], **Christopher C. Dvorak**[2], **Danna Chan**[3], **Tao Liu**[1], **Morton J. Cowan**[2], **Justin Wahlstrom**[2], **Melisa Stricherz**[4], **Cathryn Jennissen**[4], **Paul J. Orchard**[5], **Jakub Tolar**[5], **Sung-Yun Pai**[6], **Liusheng Huang**[7], **Francesca Aweeka**[3,7], and **Janel Long-Boyle**[2,3,*]

[1]Department of Pharmacy Practice and Science, University of Maryland, Maryland, Baltimore

[2]Departments of Pediatrics, University of California San Francisco, San Francisco, California

[3]Department of Clinical Pharmacy, University of California San Francisco, San Francisco, California

[4]Department of Pharmacy, University of Minnesota Masonic Children's Hospital, Minneapolis, Minnesota

[5]Division of Pediatric Blood and Marrow Transplantation, University of Minnesota, Minneapolis, Minnesota

[6]Department of Pediatrics, Boston Children's Hospital and Dana-Farber Cancer Institute, Boston, Massachusetts

[7]Drug Research Unit, Department of Clinical Pharmacy, University of California San Francisco, San Francisco, California

Abstract

A prospective multicenter study was conducted to characterize the pharmacokinetics (PK) and pharmacodynamics (PD) of fludarabine plasma (f-ara-a) and intracellular triphosphate (f-ara-ATP) in children undergoing hematopoietic cell transplantation (HCT) and receiving fludarabine with conditioning. Plasma and peripheral blood mononuclear cells (PBMCs) were collected over the course of therapy for quantitation of f-ara-a and f-ara-ATP. Nonlinear mixed-effects modeling was used to develop the PK model, including identification of covariates impacting drug disposition. Data from a total of 133 children (median age, 5 years; range, .2 to 17.9) undergoing HCT for a variety of malignant and nonmalignant disorders were available for PK-PD modeling. The implementation of allometric scaling of PK parameters alone was insufficient to describe drug clearance, particularly in very young children. Renal impairment was predicted to increase drug exposure across all ages. The rate of f-ara-a entry into PBMCs (expressed in pmoles per million cells) decreased over the course of therapy, resulting in 78% lower f-ara-ATP after the fourth dose

*Correspondence and reprint requests: Janel Long-Boyle, PharmD, PhD, Departments of Clinical Pharmacy and Pediatrics, University of California San Francisco, School of Pharmacy, 600 16th St, Genentech Hall 4N-474F, San Francisco, CA 94143. Janel.Long-Boyle@ucsf.edu (J. Long-Boyle).

Conflict of interest statement: There are no conflicts of interest to report.

(1.7 pmoles/million cells [range, .2 to 7.2]) compared with first dose (7.9 pmoles/million cells [range, .7 to 18.2]). The overall incidence of treatment-related mortality (TRM) was low at 3% and 8% at days 60 and 360, respectively, and no association with f-ara-a exposure and TRM was found. In the setting of malignancy, disease-free survival was highest at 1 year after HCT in subjects achieving a systemic f-ara-a cumulative area under the curve (cAUC) greater than 15 mg*hour/L compared to patients with a cAUC less than 15 mg*hour/L (82.6% versus 52.8% $P = .04$). These results suggest that individualized model-based dosing of fludarabine in infants and young children may reduce morbidity and mortality through improved rates of disease-free survival and limiting drug-related toxicity. ClinicalTrials.gov Identifier: NCT01316549

Keywords

Pharmacokinetics; Pharmacodynamics; Fludarabine; Pediatric; Allogeneic; Hematopoietic cell; transplantation

INTRODUCTION

Allogeneic hematopoietic cell transplantation (HCT) is used to treat a variety of pediatric disorders. Although they differ in the level of myelosuppression, many current preparative regimens are fludarabine based. Fludarabine is a nucleoside analogue used for its antileukemia activity and to enhance stem cell engraftment through its potent immunosuppressive activity against B and T lymphocytes [1,2]. Administered intravenously as a prodrug, fludarabine monophosphate (f-ara-AMP) undergoes rapid dephosphorylation in the plasma to the systemically circulating compound, f-ara-a. F-ara-a is then transported from the plasma into cells by several uptake transporters, including equilibrative nucleoside transporters (ENT1, ENT2) and the concentrative nucleoside transporters 3 [3–6]. In the cytoplasm, f-ara-a is sequentially phosphorylated to the active triphosphate species (f-ara-ATP), which inhibits DNA synthesis and RNA production, inducing apoptosis [1,2,7].

However, despite the widespread use of fludarabine, there is a lack of pharmacokinetic (PK) studies in children undergoing HCT to optimize dosing and clinical outcomes. Outside the setting of HCT, only 2 published studies reported PK data for fludarabine in children. These were phase I/II studies evaluating fludarabine administered by continuous infusion in combination with cytarabine for the treatment of relapsed leukemias and solid tumors in children [8,9]. Limited in sample size, these studies did not include very young children (<1 year of age) and were unable to sufficiently evaluate how patient-specific clinical factors may contribute to fludarabine PK variability. Furthermore, quantification of the active intracellular species, f-ara-ATP, was only performed in 4 subjects with excess white blood cells.

In adult HCT recipients, the PK of f-ara-a is variable and population PK (PopPK) analyses have identified several clinical covariates contributing significantly to drug clearance (CL), including weight and renal function, which are important clinical factors relative to children and drug exposure [10–14]. Two of the largest studies to date reported a strong association between f-ara-a exposure and risk of treatment-related adverse outcomes in adult HCT, demonstrating the need for improved dosing strategies to optimize drug therapy [11,15].

Several studies in adults with cancer or undergoing HCT for malignant disease have also attempted to define the relationship between fludarabine dose, plasma concentrations, and intracellular f-ara-ATP drug levels, with both in vitro and in vivo investigations observing large variability in intracellular concentrations of f-ara-ATP [16–23].

Understanding the relationships between f-ara-a and f-ara-ATP is critical to improving dosing strategies in children. This study's primary objective was to evaluate patient-specific factors responsible for variability in fludarabine exposure. Secondly, we aimed to identify relationships between fludarabine exposure and clinical outcomes.

PATIENTS AND METHODS

Study Population

This was a prospective PK study of fludarabine in children who underwent HCT for a variety of malignant and nonmalignant pediatric disorders. Patients were eligible to participate in PK-pharmacodynamic (PD) analysis if they were between 0 and 17.99 years old, met protocol-specific eligibility criteria for transplantation, and were to undergo an allogeneic or autologous HCT with gene therapy that included intravenous fludarabine monophosphate as part of the conditioning regimen. Patients who received fludarabine monophosphate alone or in combination with other agents given over 3 to 5 days were eligible to participate. Fludarabine PK data were collected between 2010 and 2015 at the University of California San Francisco Benioff Children's Hospital, the University of Minnesota Masonic Children's Hospital, and Boston Children's Hospital. All local institutional review boards approved this study and written informed consent/assent was obtained from all patients. The study was registered at ClinicalTrials.gov as NCT01316549.

PK Sampling

Blood collection times were selected by an optimal sampling strategy for population analysis utilizing prior f-ara-a PK data available in adults and D-optimality methods [11,24,25]. Collection times for f-ara-ATP were incorporated into the optimal sampling time based on literature estimates for time to maximum concentration and half-life [18,26]. Blood collections were performed on 2 different occasions over the course of fludarabine therapy for a total of 10 blood samples. Fludarabine was administered intravenously over 30 to 60 minutes in all patients. On the first occasion, blood samples for the quantification of f-ara-a were collected at 2, 4, 8, and 24 hours after the start of fludarabine infusion. Sampling was then repeated after a subsequent dose of fludarabine at 2 and 24 hours after the start of infusion. On both occasions, blood collection for f-ara-ATP analysis occurred at concurrent sampling times as f-ara-a (2 and 24 hours after infusion) in patients enrolled at the University of California San Francisco clinical site only (n = 66).

Plasma and intracellular drug concentrations were processed independently. For the quantification of f-ara-a in the plasma, 1 mL of whole blood was collected at each time point in a K_2 EDTA tube and placed on wet ice. All plasma samples were centrifuged at 3500 rpm for 10 minutes at 4°C within 30 minutes of collection, and the plasma was removed and stored at −70°C until analysis. Blood samples to be assayed for f-ara-ATP were collected in

a 4-mL cell preparation tube with sodium citrate and processed for recovery of peripheral blood mononuclear cells (PBMCs) as previously described [27]. For each sample, cells were stained with trypan blue and isolated PBMCs were counted using the manual hemocytometer method. Results for f-ara-ATP were normalized and presented as pmoles per million cells.

Bioanalysis of F-Ara-a and F-Ara-ATP

Plasma and PBMC samples were analyzed for f-ara-a and f-ara-ATP using 2 different validated liquid chromatography-tandem mass spectrometry methods, as previously described [28,29]. The fara-a assay was linear in the range of 2 ng/mL to 800 ng/mL. The mean accuracies (mean ± coefficient of variation) of the f-ara-a assay were 98.5% ± 7.0, 101.7% ± 6.6, and 92.8% ± 7.8 at low-, medium-, and high-quality control levels, respectively.

To measure f-ara-ATP in PBMCs, cells (~5 million) were collected and lysed with 1-mL 70% methanol containing 1.2 mM tris buffer. The lysate was mixed with an internal standard and injected into an API5000 liquid chromatography-tandem mass spectrometry system (AB SCIEX Pte. Ltd. Ontario, Canada). The linear range of the intracellular assay was 1.52 to 76 nM. The mean accuracies (mean ± coefficient of variation) were 100.7% ± 9.5, 94.0% ± 10.5, 96.3% ± 9.5 at the low-, median-, and high-quality control levels, respectively.

PopPK Analysis

A nonlinear mixed effects modeling approach using NONMEM 7.3 software (Icon Development Solutions, Hanover, MD) [30] was used to describe the time course of f-ara-a and f-ara-ATP concentrations. R software version 3.2.0 was used for graphical inspection of the results [31]. An equivalent dose of f-ara-a (molecular weight 285 g/mol) to that of the administered monophosphate form (f-ara-AMP, molecular weight 365 g/mol) was calculated and used for model building. Both f-ara-a and f-ara-ATP concentrations that fell below the lower limit of quantification were reported by the lab and entered into the model as the true value. The first-order conditional estimation method with interaction was used to estimate PK parameters and variability. Model selection was based on objective function values and goodness-of-fit plots. Residual unexplained variability was characterized separately for plasma and intracellular compartments by a proportional error model.

Covariate Modeling

Clinical data were collected on each day of PK sampling before fludarabine administration to assess the influence of patient-specific factors on f-ara-a CL. Continuous covariates that were evaluated were age, height, body surface area, creatinine clearance (CRCL), blood urea nitrogen, albumin, white blood cell count, and absolute neutrophil count. In pediatric patients, CRCL was estimated by the Schwartz method and, in young adults, by the Cockcroft-Gault equation using ideal body weight [32,33]. If the level of serum creatinine was reported back by the clinical labs as <.3 mg/dL, a value of .15 (half the limit of quantification) was used. Categorical covariates included gender, conditioning regimen, indication for transplantation, and study center. Covariate analysis was performed using a step-wise forward additive approach followed by a step-wise backward elimination approach

with an alpha of .05 and .001, respectively. The resulting final model contains only covariates that meet the predefined statistical criteria and show an acceptable precision of related parameter estimates.

Model Inclusion of F-Ara-ATP

Once a final covariate model for f-ara-a CL was selected, f-ara-ATP concentrations were linked by a clearance K_{in} that allowed transfer of drug directly from the central to the intracellular compartment. F-ara-ATP CL from PBMCs was expressed by a first-order rate constant for elimination K_{out}.

Model Evaluation

A nonparametric bootstrap resampling method was used to evaluate the stability and robustness of the final PK model. Resampling with replacement generated 1000 bootstrap datasets and the final PopPK model was fitted repeatedly to each of the 1000 bootstrap datasets. The median and 95% confidence intervals (CI) of parameters obtained from this step were compared with the final parameter estimates. In addition, the prediction-corrected visual predictive check (pcVPC), stratified by plasma and intracellular compartments with 1000 simulated datasets was also performed [34]. Results from the pcVPC were assessed using graphical comparison of the appropriate 90% prediction interval from simulated data and was visually explored with overlaid observed data from the original dataset.

Assessment of PK and Clinical Outcomes

The primary outcome for evaluating exposure-response relationships for this study was to determine the relationship between f-ara-a systemic exposure and treatment-related-mortality (TRM). *TRM* was defined as death without disease progression or relapse by day 60 and 1 year after transplantation. Secondary objectives were to evaluate the relationship between f-ara-a exposure and incidence of overall survival (OS), primary graft failure (PGF), and disease-free-survival (DFS). For OS analysis, death from any cause was considered an event. *Day of neutrophil engraftment* was defined as the first of 3 consecutive measures of an absolute neutrophil count > 500cells/uL. *PGF* was defined as alive on day 42 after transplantation with an absolute neutrophil count <500cells/uL, or the need for repeat conditioning and retransplantation within 42 days after transplantation. DFS was calculated from day of transplantation until relapse or disease progression.

Statistical Analyses for Outcomes

F-ara-a cumulative AUC (cAUC) was used as the PK metric for exposure-response analysis. Individual cAUC for each patient was derived from the empirical Bayes estimate of individual CL (AUC = dose/CL) multiplied by the total number of fludarabine doses of fludarabine received. The exploratory exposure-response analysis was performed using descriptive plots to assess the relationship of systemic f-ara-a exposure by quartiles of individual observed cAUC and TRM/PGF. Kaplan-Meier survival analysis was used to evaluate the relationship between quartiles of the individual observed cAUC and OS/DFS. Evaluation of exposure-response relationships for f-ara-ATP was not included in this analysis.

Simulations to Individualize Dosing

Based on our final PopPK model, individual f-ara-a doses were estimated using the model and compared to the conventional dosing of 40 mg/m^2. Clinical covariates for a typical patient were based on the 50th percentile estimates of weight per age as provided by the CDC standard growth charts for infants and children. Serum creatinine levels of .3 mg/dL (up to 1 year-old) and .4 mg/dL (1 to 16 years) were used as average values when estimating CRCL via the Schwartz equation for the simulated patients [32]. Based on the daily median f-ara-a $AUC_{0\text{-}24}$ for those patients receiving the most common dose level of 40 mg/m^2 in the dataset, doses of f-ara-a presented were simulated to achieve the selected AUC_{target} of 4.5 mg*hour/L (equal to a cAUC of ~ 18 mg*hour/L for 4 doses) as administered once daily over 4 days of therapy using the following equations:

$$\textit{Dose of f-ara-a (mg)} = AUC_{target} \times CL_{(individual)}$$

$$\textit{Dose of f-ara-AMP (mg)} = \textit{f-ara-a dose (mg)} \times 1.28$$

Because fludarabine is administered as the monophosphate form, the model-based dose of f-ara-a was multiplied by a factor of 1.28 to convert to f-ara-AMP dose equivalents (based on the ratio of molecular weights).

RESULTS

Patient Demographics

A total of 140 subjects completed PK assessments and were used for PK model building. Of these subjects, 7 patients were excluded from PK-PD analysis: 3 because of incomplete outcome data and 4 had undergone autologous HCT in combination with gene therapy for Wiskott-Aldrich syndrome. Patient demographics for all 133 subjects included in both PK and PD analyses are presented in Table 1. The median of time to follow-up was 313 days (range, 15 to 3084). Among the study subjects, the median age of patients was 5 years with 20% of subjects ≤12 years old. Median actual body weight was 15.7 kg and included 26% of children weighing ≤10 kg. The daily dose of fludarabine was determined on a mg/body surface area basis in 71% of subjects and on a mg/kg basis in 29% of patients.

PopPK Analysis

After inspection of the data, a total of 840 and 239 quantifiable concentrations for f-ara-a and f-ara-ATP, respectively, were available for PopPK model building (Supplemental Figure S1). A 2-compartment model for f-ara-a was found to be significantly better than a 1-compartment model ($P < .05$). A third compartment representing distribution of f-ara-a to PBMCs by a first-order rate constant K_{in} and exit rate constant K_{out} described the association of f-ara-a to f-ara-ATP. A separate additive error on the log scale for f-ara-a and f-ara-ATP was fitted to the concentration-time data. This model provided a reasonable fit of the data for both analytes and thus retained for covariate model development. The inclusion of interoccasion variability did not improve the model. A body weight-based allometric

model was added to all clearance and volume parameters for f-ara. The exploratory analysis on individual PK parameter predictions versus covariates identified CRCL as a potential covariate with a strong correlation to the CL of f-ara-a. A renal function maturation factor did not improve the model fit. No other blood chemistries or patient-specific clinical factors evaluated were found to significantly affect f-ara-a CL including indication for transplantation, conditioning regimen, or center site. Additionally, no covariates were found to affect the downstream CL of f-ara-a into the PBMCs to form f-ara-ATP or the elimination of f-ara-ATP.

The PopPK parameter estimates and their relative standard errors from the final model are presented in Table 2. The final model for f-ara-a CL incorporating weight and CRCL was follows:

$$CL_{individual} = CL_{population} \times \left(\frac{Weight}{15kg}\right)^{0.75} \times \left(\left(1 + \left(CRCL\frac{mL}{min} \Big/ 1.73m^2 - 100\right) \times CRCLEFF\right)\right)$$

where, 3.1L/hour is the typical value of f-ara-a *CL* and *CRCLEFF* represents the coefficient for the effect of CRCL on f-ara-a CL. The goodness-of-fit plots for the final model demonstrated clear improvement with good distribution of population-predicted concentration around the line of unity and there were no trends in the residuals (plots not shown). Plots displaying observed and predicted f-ara-a and f-ara-ATP drug concentrations for several representative patients are provided in Figure 1. Table 3 shows the peak and trough concentrations for f-ara-ATP. Intracellular peak concentrations decreased with time ($P < .001$). Median concentrations for f-ara-ATP decreased ~2.5 and 4.5 fold, respectively, from dose 1 of fludarabine to doses 3 and 4. A similar decrease in trough concentrations of f-ara-ATP at 24 hours after dose was shown with doses 3 and 4 ($P = .57$).

The median PK parameter estimates and 95% CIs from the bootstrap analysis are presented in Table 2. Median estimates of PK parameters, interpatient variability, and residual unexplained variability derived from the bootstrap analysis were comparable with the typical values derived from the original dataset. Standard diagnostic plots and representative model fits for individual PK profiles for f-ara-a and f-ara-ATP indicate that the model captured the data well. Additionally, the pcVPC stratified by analyte for the final covariate model (Supplemental Figure S2) shows that the variability in the data was well predicted.

Table 4 displays the derived f-ara-a $AUC_{0\text{-}24}$ values from the observed data at different dose regimens for a single 24-hour dosing interval. The median daily f-ara-a $AUC_{0\text{-}24}$ for all patients included in the analysis was 3.7 mg*hour/L (range, 3.3 to 4.5). For those patients receiving a daily dose of 40 mg/m^2, the $AUC_{0\text{-}24}$ was 4.5 mg*hour/L (range, 3.7 to 4.8). Empiric dose reductions occurred in 32% of all subjects. Specifically, for patients assigned to 40 mg/m^2/day but had empiric dose reductions (n = 38), exposure was significantly lower (3.4 mg*hour/L [range, 3.1 to 3.9] versus 4.5 mg*hour/L [range, 3.7 to 4.8], $P < .001$), indicating that comparable exposure was not achieved with the current strategy.

Patient-specific covariates found to impact f-ara-a CL were actual body weight and CRCL. Figure 2 shows the model-predicted dose of f-ara-AMP for children of different ages and

renal function. Based on the daily median f-ara-a AUC_{0-24} for those patients receiving the most common dose level of 40 mg/m^2 in the dataset, doses of f-ara-AMP were simulated to achieve the selected daily AUC_{0-24} of 4.5 mg*hour/L administered once daily over 4 days of therapy (equal to a cAUC of 18 mg*hour/L). Levels of renal function were selected based on regulatory guidelines for PK studies in patients with impaired renal function. The model demonstrates that regardless of age and renal impairment, dose modifications are needed to avoid elevated drug exposure (Figure 2A). Simulated CL values suggest that for children ≤ 6 months of age, dose reductions are required to provide exposure comparable to older children (Figure 2B). For example, the model-predicted dose for a 4.5-month-old-child weighing 7 kg with normal renal function for age would be 8.8 mg per dose, which is a 37% dose reduction compared with a traditional dose of 40 mg/m^2/dose or a 4.5% dose reduction from a dose of 1.3 mg/kg/dose.

Exposure and Relationships with Outcomes

The primary endpoint for this study was to determine the relationship between f-ara-a exposure and TRM. The overall incidences of TRM were 3% and 8% at days 60 and 360, respectively, with a median time to death of 66 days (range, 15 to 163). No association between f-ara-a exposure and TRM was found with a median f-ara-a cAUC for all subjects with TRM at 1 year (n = 10) of 16 mg*hour/L (range, 7.6 to 39.0) compared with 11 mg*hour/L (range, 8.9 to 22.3) in patients without TRM ($P = .35$). Of the 10 children who died by 1 year after HCT, 7 underwent allogeneic HCT for a nonmalignant diagnosis with a median f-ara-a cAUC of 16.3 mg*hour/L (range, 10.7 to 33.8). The median age for these 7 subjects was younger at .92 years (range, .33 to 9) compared with 2 years (range, .2 to 17.0) in surviving nonmalignant patients ($P = .57$). The cause of death included end-organ pulmonary or renal failure (n = 8) and infection (n = 2).

OS—At days 60 and 360, OS rates were 95% and 78%, respectively. Figure 3A shows the proportion of patients surviving plotted by observed f-ara-cAUC quartiles, regardless of diagnosis. The highest 1-year OS rate was observed in patients with a cAUC ranging from 15 mg*hour/L to 19 mg*hour/L. Figure 3B shows the Kaplan-Meier curves for the population stratified by malignant or nonmalignant diagnosis. OS at 1 year was lower in patients with a malignant diagnosis at 67% (95% Cl, 55% to 82%) compared with those with a nonmalignant disease at 85% (95% Cl, 77% to 94%; $P = .046$). For patients with nonmalignant disease, there was no trend of OS at 1 year after HCT with increasing f-ara-a exposure ($P = .60$) (Figure 4).

DFS—A total of 59 (44%) out of 133 subjects included in PK-PD analysis had malignant disease and were eligible for analysis of DFS. The rates of DFS in patients with the diagnosis of a malignant disorder were 86% and 62% at days 60 and 360 after HCT, respectively. Figure 5A shows proportion of patients with DFS by observed f-ara-a cAUC quartiles. The highest proportion of patients experiencing DFS at 1 year after HCT was observed in patients with a cAUC ranging from 15 mg*hour/L to 19 mg*hour/L. In subjects achieving a cAUC >15 mg*hour/L, DFS was higher at ~82.6%, compared with patients with a cAUC <15 mg*hour/L at 52.8% ($P = .04$). Median cAUC for the third and fourth quartiles were 16.6 mg*hour/L (range, 15.2 to 18.5) and 23.6 mg*hour/L (range, 19.1 to 39.0),

respectively. Corresponding survival curves for the proportion of patients with DFS at 1 year after HCT stratified by f-ara-a cAUC quartiles are shown in Figure 5B.

Of the 74 subjects with nonmalignant diagnoses, only 2 patients required a second transplantation within day 100 after HCT. Thus, no formal testing between f-ara-a cAUC and DFS in this group was performed.

PGF—The median time to neutrophil engraftment was 15 days (range, 5 to 148). PGF occurred in 9 subjects (3 malignant, 6 nonmalignant). There was a trend towards higher incidence of PGF in patients receiving mg/kg once daily dosing than in patients receiving 40 mg/m^2/day (13% versus 4%), although the trend was nonsignificant (.117). Patients experiencing PGF had lower f-ara-a exposure when dosed on a mg/kg basis compared with subjects receiving 40 mg/m^2/day (cAUC of 13.9 mg*hour/L [range, 8.0 to 16.3] versus 18.6 mg*hour/L [range, 7.7 to 21.5], $P < .001$).

Minimum Exposure Threshold

Using evidence from all the exploratory exposure-response analysis and the OS and DFS proportions by cAUC quartiles (Figures 3 and 5), a cAUC > 15 mg*hour/L was considered an adequate minimum threshold to achieve the best possible outcome given the data obtained in this study. Proportion of DFS below and above this threshold of 15 mg*hour/L are significantly different ($P = .04$). No inferences on toxicity could be made from likely because of empiric dose reductions and low number of events in this observational study.

DISCUSSION

The unique developmental aspects of PK-PD in children, especially in neonates and infants, are now well recognized [35]. Understanding the effects of growth and maturation on PK and PD variability is critical to optimize pediatric dose selection. Older children and adolescent PK studies typically demonstrate a high correlation between body size and age [36]. Thus, for children >2 years of age, allometric scaling is sufficient to accurately reflect the impact of body size and age on drug disposition. However, for infants and younger children, the incorporation of organ function/maturation are required to accurately predict PK [37]. Therefore, the inclusion of allometric scaling in our model accounts for changes in drug CL due to body size, and the inclusion of CRCL accounts for renal function, which is highly correlated with age. Particularly for children ages <6 months, the model suggests significant dose reductions are necessary to achieve exposure comparable to older children with the same exposure target. Empiric dose reductions aimed to account for younger age or low weight (mg/kg) led to significantly lower exposure, indicating that the current strategies are inadequate and may lead to suboptimal f-ara-a exposure.

The addition of CRCL as a predictor of f-ara-a CL was not unexpected considering f-ara-a undergoes extensive renal elimination through a combination of glomerular filtration and active tubular secretion [26]. In adult allogeneic HCT, the total body CL of the systemically circulating metabolite f-ara-a is known to correlate well with CRCL, indicating the importance of renal excretion for the elimination of the drug [11,15,38,39]. Based on our final model, the predicted CL of f-ara-a in children >15 years of age was approximately 11

L/hour and compares well with the previously reported CL of f-ara-a in adult HCT recipients [11,15]. Current guidelines published by the manufacturer recommend a nonspecific 20% dose reduction in adult patients with moderate renal impairment and not recommended for patients with CRCL<30 mL/minute [15,38,39]. Model simulations demonstrate that in the presence of renal impairment dose, modifications in children are needed to avoid elevated drug exposure. Of note, using serum creatinine and the Schwartz equation may lead to overestimation of renal function in the pediatric population. However, the rationale for using this method was based on our historical experience that the ability to successfully recruit pediatric HCT patients is significantly hampered when urine collections or more invasive methods (eg, nuclear glomerular filtration rate studies) are required for PK studies. Furthermore, use of urinary catheters poses serious risk for infection in neutropenic patients.

This is the first published report investigating the PK of the active species f-ara-ATP in clinical samples collected in a pediatric allogeneic HCT population. Several studies in adults have attempted to define the relationship between fludarabine dose, plasma concentrations, and intracellular f-ara-ATP drug levels [26]. In vitro and in vivo investigations have reported wide interpatient variability in intracellular concentrations of f-ara-ATP in several different subsets of T lymphocytes [16–22]. One study suggests a linear relationship between fludarabine dose, f-ara-a plasma concentrations, and increased accumulation of f-ara-ATP in leukemic blasts [26]. Our results are in agreement with previous studies demonstrating significant interpatient variability in both peak and trough levels of f-ara-ATP. However, the results are inconsistent with those previously reported in adults, as we demonstrate intracellular drug exposure represented by f-ara-ATP peaks and troughs in PBMCs decline with repeat consecutive daily dosing. Several major differences in study design may account for differences between our results and previous reports. First, we quantify f-ara-ATP in clinical samples of purified PBMCs after fludarabine treatment as compared with pretreatment collection of cells and ex vivo incubation with fludarabine. Secondly, f-ara-ATP levels in our study were evaluated on 2 different occasions over the course of fludarabine therapy, allowing for evaluation of changes in drug levels within an individual over time. These results indicate that fludarabine may have saturable accumulation of f-ara-ATP within target cells, possibly through inhibition of membrane transporters or enzymes involved in the disposition and metabolism of f-ara-a as demonstrated by gemcitabine, a nucleoside analogue with shared metabolic pathways [40,41]. Lastly, the disposition of f-ara-ATP may be highly variable among different patient populations and disease subsets. Presumed assumptions in similarities between intracellular exposure for malignant populations, such as chronic lymphocytic leukemia, and nonmalignant disorders, such as the primary immune deficiencies or leukodystrophies may not be appropriate. Further refinement of the analytical methods and evaluation of specific T cell populations to evaluate the optimal plasma concentration of f-ara-a that facilitates the maximum rate of formation of f-ara-ATP within cells, along with how the rate of drug infusion impacts intracellular exposure are ongoing. Additionally, f-ara-ATP concentrations were not evaluated for PD endpoints, which are currently being investigated by our group.

The subjects evaluated in this analysis represent a more heterogeneous population regarding disease and conditioning compared with evaluations of fludarabine PK-PD in adult allogeneic HCT. Thus, the ability to define exposure-response relationships is more

challenging. Given our sample size of 133 patients, we found no association between f-ara-a $AUC_{0\text{-}24}$ or cAUC and TRM. This is in contrast to several recent clinical investigations in adult allogeneic HCT where higher risk of TRM or nonrelapse mortality was associated with a daily f-ara-a $AUC_{0\text{-}24}$ ranging from approximately 5 mg*hour/L to 7 mg*hour/L (doses ranged from 40 mg/m^2/day to 50 mg/m^2/day over 5 days of therapy) [11,15,42]. Compared with these studies, the incidence of TRM among our patient population was low at 1 year after HCT. Reflective of wider range of fludarabine dose and empiric dose reductions in nearly one-third of the patients studied, the average daily $AUC_{0–24}$ in our study was lower at 3.7 mg*hour/L, versus 4.9 mg*hour/L in adults receiving fludarabine dosed at 40 mg/m^2 once daily as estimated by similar PK methodologies [11,15]. The lower exposure and incidence of TRM compared with those for adults indicate that the threshold for drug levels that lead to drug-related toxicity may not be typically exceeded in a pediatric population, when young age or kidney function are taken into account to determine initial doses. Our PopPK model demonstrated that f-ara-a drug exposure is a function of patient-specific covariates. This signifies an important shift in the paradigm of fludarabine dosing, away from predefined dose intensity (eg, 25 mg/m^2 or 40 mg/m^2 over 4 days) to a tailored individualized approach to therapy. With recent advancements, model-based dosing can be implemented into clinical protocols and used to individualize therapy irrespective of the therapeutic target or number of doses.

Our results indicate that different therapeutic targets may be appropriate to optimize fludarabine therapy among patients, particularly in children with malignant diagnoses. Because fludarabine is pharmacologically active against a variety of hematologic malignancies, its utility in the preparative regimens of allogeneic HCT is considered 2 fold. First, fludarabine synergizes with other high-dose chemotherapeutic agents to eliminate tumor cells. Second, it facilitates donor stem cell engraftment to allow the development of a graft-versus-leukemia effect.

For both OS and DFS, the highest probability of a positive outcome was among patients with a cAUC between 15 mg*hour/L and 19 mg*hour/L. Based on our PK-PD results, achieving an f-ara-a cAUC >15 mg*hour/L in the setting of malignancy may enhance the antineoplastic properties of fludarabine and support the graft-versus-leukemia effect. Achieving this level of targeted exposure over 4 to 5 days of therapy is feasible with model-based dosing to maintain daily exposures under the upper threshold for drug-related toxicity or nonrelapse mortality as seen in adult allogeneic HCT ($AUC_{0\text{-}24}$ 5 mg*hour/L to 7 mg*hour/L) [11,15,42]. However, courses of fludarabine therapy aimed to achieve a cAUC >15 mg*hour/L and shorter than 4 days should be avoided because of higher daily exposures, which have been associated with increased TRM in adults.

In the setting of allogeneic HCT for the treatment of non-malignant conditions, the relationship between f-ara-a cAUC is less clear and optimization of dosing to achieve a specific exposure requires further evaluation. There was no observed trend for OS at 1 year after HCT in patients with nonmalignant disease. However, nonmalignant conditions are more variable in respect to their degree of graft resistance as well as their tolerance of chemotherapy. The number of subjects experiencing PGF in this study was small and, therefore, more patients in each disease group will be required to determine if there is an

optimal dose of f-ara-a exposure that supports engraftment while minimizing toxicity. The effects of combination chemotherapy, including a comprehensive evaluation of all drug exposure expected to influence engraftment must also be considered. Of note, we did test for the impact of regimen on the CL of f-ara-a and it was not found to be significant. A continuation of this work between institutions is required to increase sample size of subpopulations and enhance our ability to refine PK-PD relationships in the setting of transplantation for nonmalignant disease.

Although the PK parameters were well estimated by our final model for f-ara-a and f-ara-ATP, the residual unexplained variability remains approximately 25% and 72%, respectively, suggesting other factors not tested in this analysis may be important determinants of fludarabine exposure and disposition. One potential factor unexplored includes genetic variants of genes involved in fludarabine metabolism and disposition. Significant interindividual variability in the gene expression of transporters and enzymes involved in fludarabine uptake and activation to f-ara-ATP has been reported in healthy volunteers and chronic lymphocytic leukemia patients [5,21,22,43]. Single nucleotide polymorphisms involved in the metabolic pathway of nucleoside analogues have been identified and are postulated to influence drug exposure [44–47]. ENT1, ENT2, and concentrative nucleoside transporter 3 have been shown to influence in vitro distribution and accumulation of fludarabine [3,4,6]. These transporters are expressed in both target tissues and renal epithelial cells of the kidney and may impact drug exposure and disposition through several mechanisms [48,49].

CONCLUSION

To date, this work represents the largest and most comprehensive study of fludarabine pharmacology in pediatric patients undergoing HCT. Before this analysis, the role of patient-specific factors on fludarabine exposure had not yet been investigated children. Our covariate analysis revealed actual body weight and CRCL to be significant patient-specific factors affecting f-ara-a CL. The final PopPK model predicts f-ara-a exposure is the highest in very young children or those with pre-existing renal dysfunction. Moving away from traditional dosing intensity strategies to model-based dosing allows for tailored drug exposure. Further development of model-based dosing in this setting has the potential to minimize toxicity while maximizing efficacy, resulting in superior outcomes for malignant and non-malignant patients alike.

Supplementary Material

Refer to Web version on PubMed Central for supplementary material.

ACKNOWLEDGMENTS

The authors thank all the patients, families, nursing and support staff for their contributions to this study.

Financial disclosure: This work was supported by an Early Career Award through the Thrasher Research Fund and the National Center for Advancing Translational Sciences, National Institutes of Health, through UCSF-CTSI Grant Number KL2 TR000143 (JLB). Funding from NIH Grant U54 AI 082973 supported MJC, CCD, and SYP. SYP was supported by the National Heart, Lung, and Blood Institute (NHLBI) Gene Therapy Resource Program (GTRP)

contract HHSM2682012000021. Its contents are solely the responsibility of the authors and do not necessarily represent the official views of the NIH.

REFERENCES

1. Dow LW, Bell DE, Poulakos L, Fridland A. Differences in metabolism and cytotoxicity between 9-beta-D arabinofuranosyladenine and 9-beta-D-arabinofuranosyl-2-fluoroadenine in human leukemic lymphoblasts. Cancer Res. 1980;40:1405–1410. [PubMed: 6245791]
2. Brockman RW, Cheng YC, Schabel FM, Jr, Montgomery JA. Metabolism and chemotherapeutic activity of 9-beta-D-arabinofuranosyl-2-fluoroadenine against murine leukemia L1210 and evidence for its phosphorylation by deoxycytidine kinase. Cancer Res. 1980;40:3610–3615. [PubMed: 6254636]
3. Ritzel MW, Ng AM, Yao SY, et al. Molecular identification and characterization of novel human and mouse concentrative Na+-nucleoside cotransporter proteins (hCNT3 and mCNT3) broadly selective for purine and pyrimidine nucleosides (system cib). J Biol Chem. 2001;276:2914–2927. [PubMed: 11032837]
4. Molina-Arcas M, Bellosillo B, Casado FJ, et al. Fludarabine uptake mechanisms in B-cell chronic lymphocytic leukemia. Blood. 2003;101:2328–2334. [PubMed: 12411296]
5. Mackey JR, Galmarini CM, Graham KA, et al. Quantitative analysis of nucleoside transporter and metabolism gene expression in chronic lymphocytic leukemia (CLL): identification of fludarabine-sensitive and -insensitive populations. Blood. 2005;105:767–774. [PubMed: 15454483]
6. Elwi AN, Damaraju VL, Kuzma ML, et al. Transepithelial fluxes of adenosine and 2'-deoxyadenosine across human renal proximal tubule cells: roles of nucleoside transporters hENT1, hENT2, and hCNT3. Am J Physiol Renal Physiol. 2009;296:F1439–F1451. [PubMed: 19297449]
7. Plunkett W, Huang P, Gandhi V. Metabolism and action of fludarabine phosphate. Semin Oncol. 1990;17(5 suppl 8):3–17.
8. Avramis VI, Wiersma S, Krailo MD, et al. Pharmacokinetic and pharmacodynamic studies of fludarabine and cytosine arabinoside administered as loading boluses followed by continuous infusions after a phase I/II study in pediatric patients with relapsed leukemias. The Children's Cancer Group. Clin Cancer Res. 1998;4:45–52. [PubMed: 9516951]
9. Avramis VI, Champagne J, Sato J, et al. Pharmacology of fludarabine phosphate after a phase I/II trial by a loading bolus and continuous infusion in pediatric patients. Cancer Res. 1990;50:7226–7231. [PubMed: 1699658]
10. Bornhauser M, Storer B, Slattery JT, et al. Conditioning with fludarabine and targeted busulfan for transplantation of allogeneic hematopoietic stem cells. Blood. 2003;102:820–826. [PubMed: 12676781]
11. Long-Boyle JR, Green KG, Brunstein CG, et al. High fludarabine exposure and relationship with treatment-related mortality after nonmyeloablative hematopoietic cell transplantation. Bone Marrow Transplant. 2011;46:20–26. [PubMed: 20383215]
12. Salinger DH, Blough DK, Vicini P, et al. A limited sampling schedule to estimate individual pharmacokinetic parameters of fludarabine in hematopoietic cell transplant patients. Clin Cancer Res. 2009;15:5280–5287. [PubMed: 19671874]
13. Bonin M, Pursche S, Bergeman T, et al. F-ara-A pharmacokinetics during reduced-intensity conditioning therapy with fludarabine and busulfan. Bone Marrow Transplant. 2007;39:201–206. [PubMed: 17211431]
14. Baron K. Longboyle J. Jacobson P. Brunstein C. Weisdorf D. Brundage R. Pharmacometric basis for a fludarabine test dose strategy in nonmyeloablative hematopoietic stem cell transplantation; Abstracts for the American Conference on Pharmacometrics; Mashantucket, CT: 2009. Available at: http://www.acop8.org/assets/Legacy_ACOPs/2009ACOP/2009%20acop%20program%202.pdf
15. Sanghavi K, Wiseman A, Kirstein MN, et al. Personalized fludarabine dosing to reduce nonrelapse mortality in hematopoietic stem-cell transplant recipients receiving reduced intensity conditioning. Transl Res. 2016;175:103–115. [PubMed: 27094990]
16. Danhauser L, Plunkett W, Keating M, Cabanillas F. 9-beta-D-arabinofuranosyl-2-fluoroadenine 5'-monophosphate pharmacokinetics in plasma and tumor cells of patients with relapsed leukemia and lymphoma. CancerChemotherPharmacol. 1986;18:145–152.

17. Malspeis L, Grever MR, Staubus AE, Young D. Pharmacokinetics of 2-F-ara-A (9-beta-D-arabinofuranosyl-2-fluoroadenine) in cancer patients during the phase I clinical investigation of fludarabine phosphate. Semin Oncol. 1990;17(5 suppl 8):18–32.
18. Danhauser L, Plunkett W, Liliemark J, Gandhi V, Iacoboni S, Keating M. Comparison between the plasma and intracellular pharmacology of 1-beta-D-arabinofuranosylcytosine and 9-beta-D-arabinofuranosyl-2-fluoroadenine 5'-monophosphate in patients with relapsed leukemia. Leukemia. 1987;1:638–643. [PubMed: 3478543]
19. Gandhi V, Kemena A, Keating MJ, Plunkett W. Cellular pharmacology of fludarabine triphosphate in chronic lymphocytic leukemia cells during fludarabine therapy. Leuk Lymphoma. 1993;10:49–56. [PubMed: 8374523]
20. Gandhi V, Estey E, Du M, Keating MJ, Plunkett W. Minimum dose of fludarabine for the maximal modulation of 1-beta-D-arabinofuranosylcytosine triphosphate in human leukemia blasts during therapy. Clin Cancer Res. 1997;3:1539–1545. [PubMed: 9815841]
21. Woodahl EL, Wang J, Heimfeld S, Sandmaier BM, McCune JS. Intracellular disposition of fludarabine triphosphate in human natural killer cells. Cancer ChemotherPharmacol. 2009;63:959–964.
22. Woodahl EL, Wang J, Heimfeld S, et al. A novel phenotypic method to determine fludarabine triphosphate accumulation in T-lymphocytes from hematopoietic cell transplantation patients. Cancer Chemother Pharmacol. 2009;63:391–401. [PubMed: 18398611]
23. McCune JS, Mager DE, Bemer MJ, Sandmaier BM, Storer BE, Heimfeld S. Association of fludarabine pharmacokinetic/dynamic biomarkers with donor chimerism in nonmyeloablative HCT recipients. CancerChemother Pharmacol. 2015;76:85–96.
24. Bazzoli C, Retout S, Mentre F. Design evaluation and optimisation in multiple response nonlinear mixed effect models: PFIM 3.0. Comput Methods Programs Biomed. 2010;98:55–65. [PubMed: 19892427]
25. Baron KLJ, Jacobson P, Brunstein C, Weisdorf D, Brundage R. March 2009). Pharmacometric Basis for a Fludarabine Test Dose Strategy in Non-myeloablative Hematopoietic Stem Cell Transplantation Abstracts for the American Conference on Pharmacometrics. Available at: http://www.acop7.org/previous-acop-meetings-acop-2009-posters.
26. Gandhi V, Plunkett W. Cellular and clinical pharmacology of fludarabine. Clin Pharmacokinet. 2002;41:93–103. [PubMed: 11888330]
27. Aweeka FT, Kang M, YuJ Y, Lizak P, Alston B, Chung RT Pharmacokinetic evaluation of the effects of ribavirin on zidovudine triphosphate formation: ACTG 5092s StudyTeam. HIVMed. 2007;8:288–294.
28. Huang L, Lizak P, Dvorak CC, Aweeka F, Long-Boyle J. Simultaneous determination of fludarabine and clofarabine in human plasma by LC-MS/MS. J Chromatogr B Analyt Technol Biomed Life Sci. 2014;960:194–199.
29. Huang L, Lizak P, Aweeka F, Long-Boyle J. Determination of intracellular fludarabine triphosphate in human peripheral blood mononuclear cells by LC-MS/MS. JPharm BiomedAnal. 2013;86:198–203.
30. Lindbom L, Pihlgren P, Jonsson EN. PsN-Toolkit–a collection of computer intensive statistical methods for non-linear mixed effect modeling using NONMEM. Comput Methods Programs Biomed. 2005;79: 241–257. [PubMed: 16023764]
31. R: A language and environment for statistical computing Vienna, Austria: R Foundation for Statistical Computing; 2010.
32. Schwartz GJ, Gauthier B. A simple estimate of glomerular filtration rate in adolescent boys. J Pediatr. 1985;106:522–526. [PubMed: 3973793]
33. Cockcroft DW, Gault MH. Prediction of creatinine clearance from serum creatinine. Nephron. 1976;16:31–41. [PubMed: 1244564]
34. Bergstrand M, Hooker AC, Wallin JE, Karlsson MO Prediction-corrected visual predictive checks for diagnosing nonlinear mixed-effects models. AAPSJ. 2011;13:143–151. [PubMed: 21302010]
35. Askie L, Offringa M. Systematic reviews and meta-analysis. Semin Fetal Neonatal Med. 2015;20:403–409. [PubMed: 26515266]

36. Meibohm B, Laer S, Panetta JC, Barrett JS. Population pharmacokinetic studies in pediatrics: issues in design and analysis. AAPS J. 2005;7:E475–E487. [PubMed: 16353925]
37. Holford N, Heo YA, Anderson B. A pharmacokinetic standard for babies and adults. J Pharm Sci. 2013;102:2941–2952. [PubMed: 23650116]
38. Anonymous. Product Information: Fludara (R) (fludarabine phosphate) For Injection. Richmond, CA: Berlex Laboratories; 2002.
39. Lichtman SM, Etcubanas E, Budman DR, et al. The pharmacokinetics and pharmacodynamics of fludarabine phosphate in patients with renal impairment: a prospective dose adjustment study. Cancer Invest. 2002;20:904–913. [PubMed: 12449721]
40. Ciccolini J, Serdjebi C, Peters GJ, Giovannetti E. Pharmacokinetics and pharmacogenetics of Gemcitabine as a mainstay in adult and pediatric oncology: an EORTC-PAMM perspective. Cancer Chemother Pharmacol. 2016;78:1–12. [PubMed: 27007129]
41. Grunewald R, Abbruzzese JL, Tarassoff P, Plunkett W. Saturation of 2',2'-difluorodeoxycytidine 5'-triphosphate accumulation by mononuclear cells during a phase I trial of gemcitabine. Cancer Chemother Pharmacol. 1991;27:258–262. [PubMed: 1998982]
42. McCune JS, Woodahl EL, Furlong T, et al. A pilot pharmacologic biomarker study of busulfan and fludarabine in hematopoietic cell transplant recipients. Cancer Chemother Pharmacol. 2012;69:263–272. [PubMed: 21909959]
43. Molina-Arcas M, Marce S, Villamor N, et al. Equilibrative nucleoside transporter-2 (hENT2) protein expression correlates with ex vivo sensitivity to fludarabine in chronic lymphocytic leukemia (CLL) cells. Leukemia. 2005;19:64–68. [PubMed: 15510196]
44. Badagnani I, Chan W, Castro RA, et al. Functional analysis of genetic variants in the human concentrative nucleoside transporter 3 (CNT3; SLC28A3). Pharmacogenomics J. 2005;5:157–165. [PubMed: 15738947]
45. Owen RP, Lagpacan LL, Taylor TR, et al. Functional characterization and haplotype analysis of polymorphisms in the human equilibrative nucleoside transporter, ENT2. Drug Metab Dispos. 2006;34:12–15. [PubMed: 16214850]
46. Lamba JK, Crews K, Pounds S, et al. Pharmacogenetics of deoxycytidine kinase: identification and characterization of novel genetic variants. J Pharmacol Exp Ther. 2007;323:935–945. [PubMed: 17855478]
47. Lamba JK. Genetic factors influencing cytarabine therapy. Pharmacogenomics. 2009;10:1657–1674. [PubMed: 19842938]
48. Mangravite LM, Badagnani I, Giacomini KM. Nucleoside transporters in the disposition and targeting of nucleoside analogs in the kidney. Eur J Pharmacol. 2003;479:269–281. [PubMed: 14612157]
49. Mangravite LM, Xiao G, Giacomini KM. Localization of human equilibrative nucleoside transporters, hENT1 and hENT2, in renal epithelial cells. Am J Physiol Renal Physiol. 2003;284:F902–F910. [PubMed: 12527552]

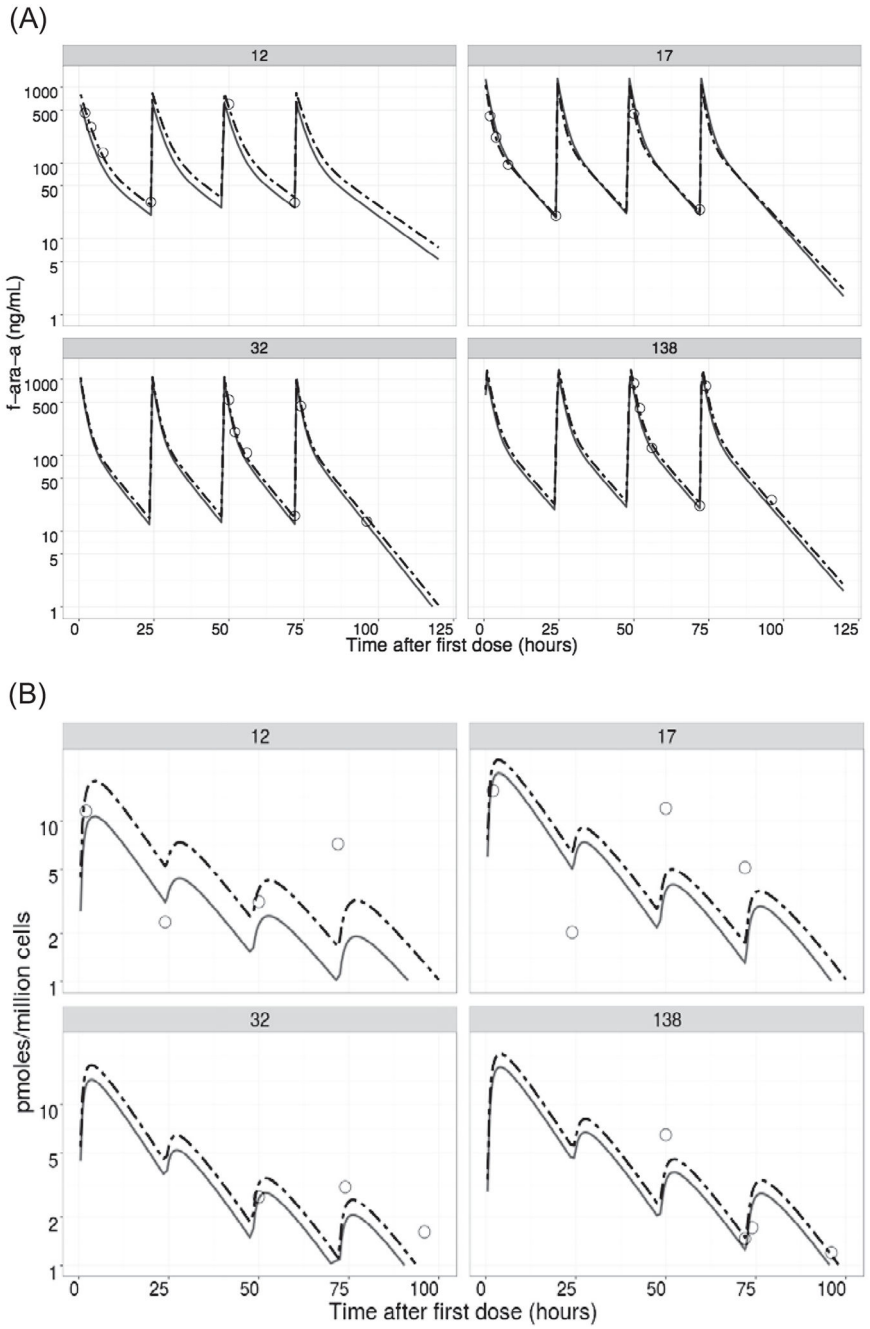

Figure 1.

Individual fit plots of observed and predicted time concentration data of (A) f-ara-a and (B) f-ara-ATP for several representative patients. Open circles represent the observed concentrations, black solid line is the population prediction, and the dashed line is the individual prediction.

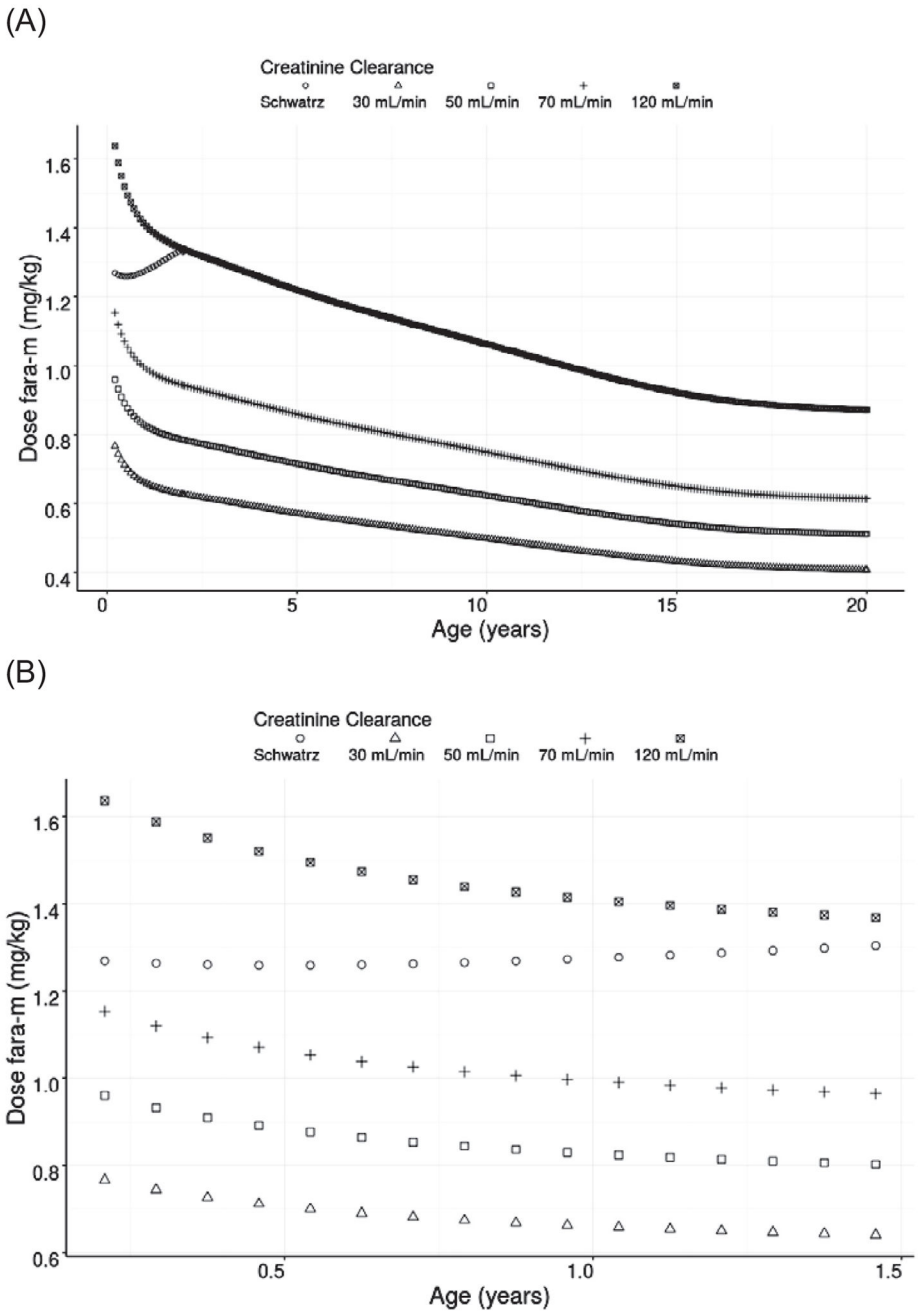

Figure 2.

Model-predicted dose of fludarabine in mg/kg aimed to achieve an daily AUC target of 4.5 mg*hour/L for (A) ages .2 to 20 years of age with varying degrees of renal function and (B) ages 0 to 2 years of age with varying degrees of renal function.

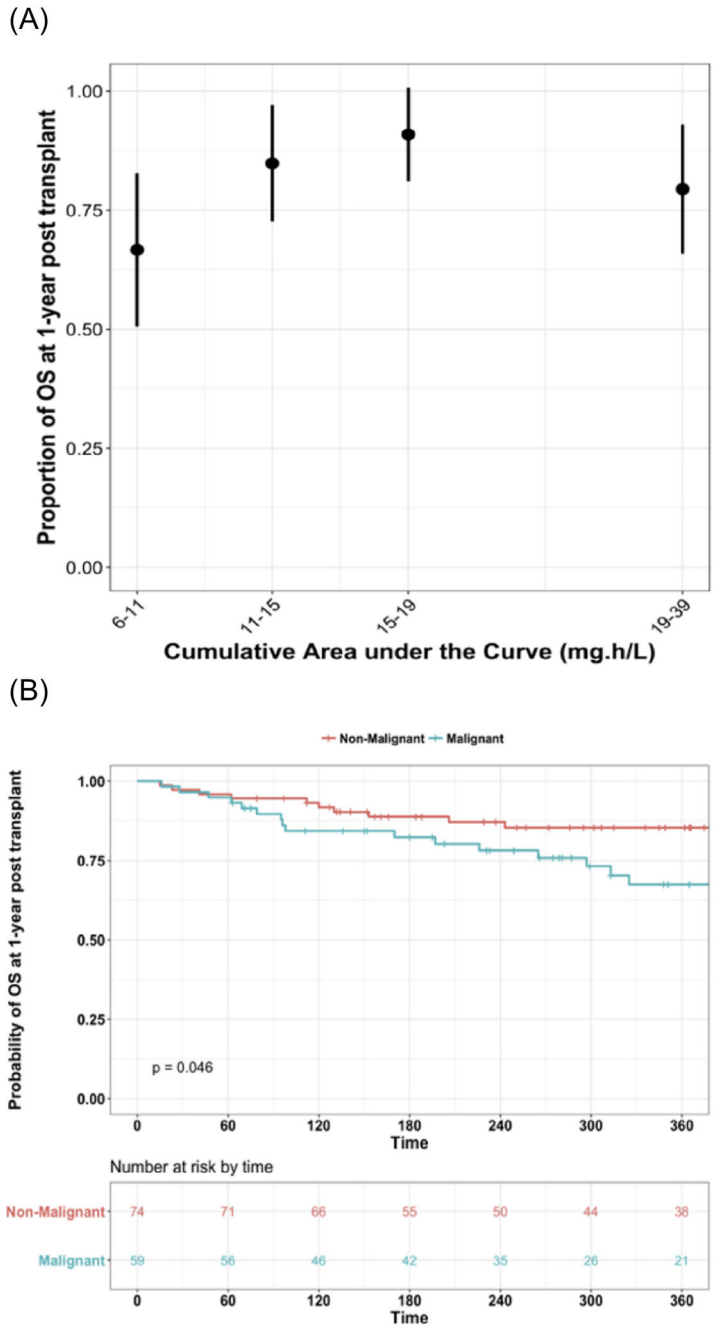

Figure 3.

OS for all subjects at 1 year after HCT. (A) Shows the proportion of patients surviving plotted by observed f-ara- cAUC quartile and regardless of diagnosis. (B) displays the OS stratified by malignant or nonmalignant diagnosis.

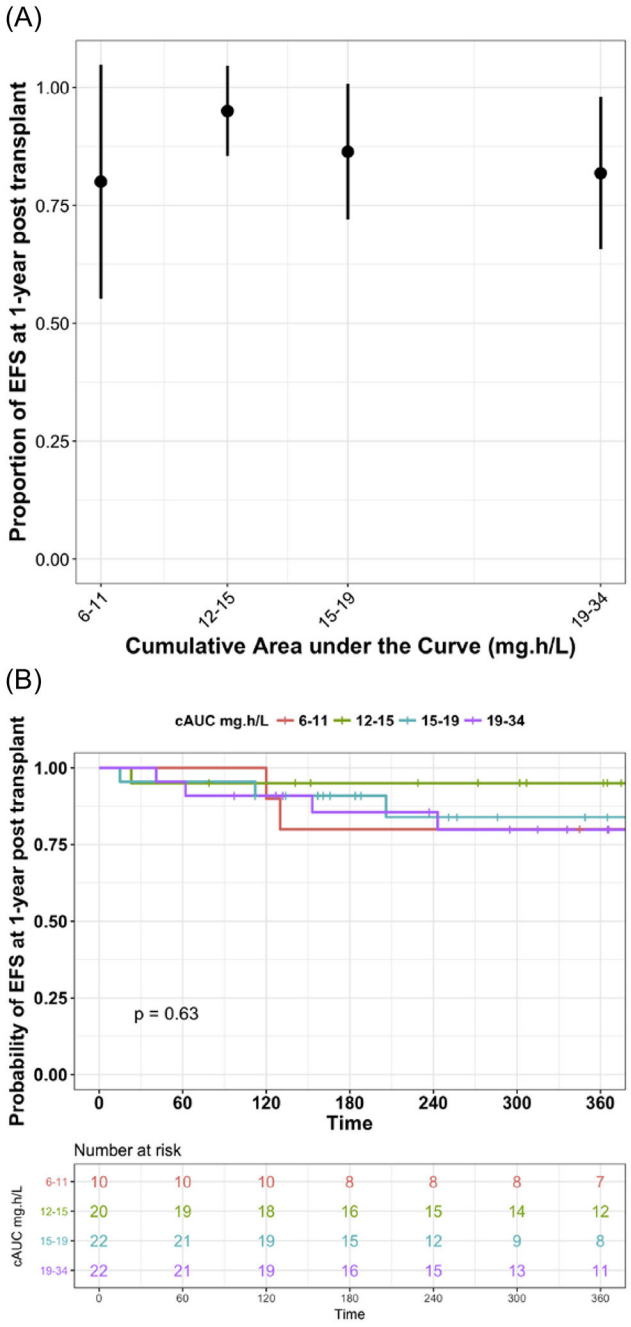

Figure 4.

OS at 1 year after HCT for patients with a nonmalignant diagnosis presented by f-ara-a cAUC quartiles.

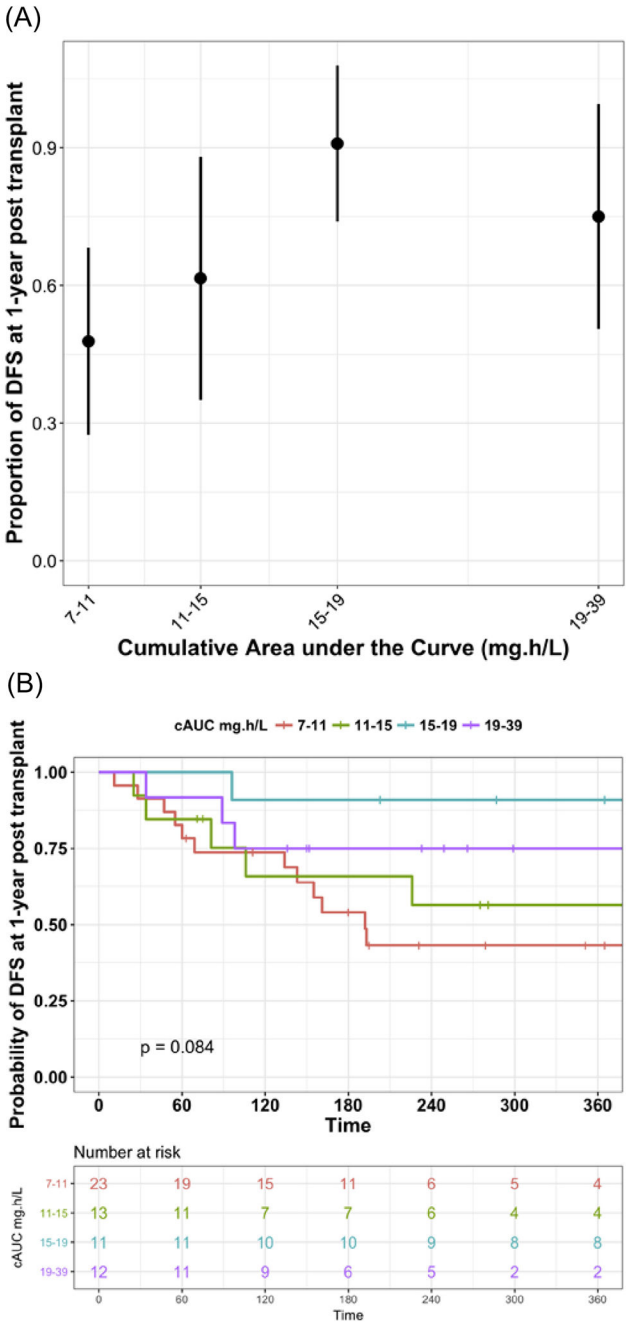

Figure 5.

DFS in patients with malignant disease only at 1 year after HCT. (A) Shows box plots of the proportion of patients with DFS by observed f-ara- cAUC quartiles. (B) Displays survival curves for the proportion of patients with DFS stratified by f-ara-a cAUC quartiles of observed data.

Table 1

Patient Demographics and Baseline Characteristics *

Characteristic	Value
No. of subjects	133
Female/male	61 (46%)/72 (54%)
Age, median (range), yr	5.0 (.2-17.9)
Weight, median (range), kg	15.7 (3-111)
Body surface area, median (range), m^2	.68 (.2-2.3)
Serum creatinine, median (range), mg/dL	.3 (.14-1.89)
Creatinine clearance, median (range), mL/min/m^2 †	150 (35-150)
Diagnosis	
Hematologic malignancies	59 (44%)
Primary immune deficiencies	18 (14%)
Hemoglobinopathies	8 (6%)
Inherited metabolic disorders	22 (16%)
Bone marrow failure	22 (16%)
Epidermolysis bullosa	4 (4%)
Conditioning regimen	
Busulfan/fludarabine	40 (30%)
Cyclophosphamide/fludarabine	45 (34%)
Busulfan/fludarabine/clofarabine	18 (14%)
Fludarabine/thiotepa/melphalan	15 (11%)
Other	15 (11%)
Serotherapy	
Antithymocyte globulin	60 (45%)
Alemtuzumab	33 (25%)
None	40 (30%)
Donor relation	
Related	38 (29%)
Unrelated	95 (71%)
Donor Source	
Bone marrow	62 (47%)
Umbilical cord blood	38 (29%)
Peripheral blood stem cells	33 (24%)
Degree of HLA mismatch	
Bone marrow or peripheral blood	
Fully matched	44 (46%)
1 Degree mismatch	36 (38%)
≥ 2 Degrees mismatch	15 (16%)
Umbilical Cord	
Fully matched	11 (29%)
1 Degree mismatch	21 (55%)

Characteristic	Value
≥ 2 Degrees mismatch	6 (16%)
Fludarabine daily dose	
40 mg/m^2	55 (41%)
12.5-35 mg/m^2	40 (30%)
.9-1.33 mg/kg	38 (29%)

Data presented are n (%) unless otherwise indicated.

* Laboratory data was collected just prior to the first dose of fludarabine.

† Creatinine clearance was estimated in children using the Schwartz method and in young adults greater than 17 years of age by the Cockcroft-Gault equation using ideal body weight.

Table 2

Final PopPK Model Parameter Estimates and Bootstrap Results

	Final Model Results		Bootstrap Results	
Population PK Parameters	**Parameter Estimates**	**RSE***	**Median Value**	**95% CI**
Typical value forf-ara-a CL, L/h/15 kg	3.1	3.3	3.1	2.9-3.4
Effect of creatinine clearance on f-ara-a CL	.006	9.5	.006	.004-.008
Vc, L/kg	13.4	6.3	13.4	11.9-14.9
Intercompartmental CL, L/h/kg	2.2	10.4	2.20	1.8-2.6
Vp, L/15	13.4	4.8	13.3	12.3-14.4
K_{in} †	.005	15.4	.005	.004-.008
Time effect on kin	−.41	12.7	−.41	−.52-−.30
K_{out} ‡	.09	7.2	.09	.08-.10
Interindividual variability on CL§ (% shrinkage)	31.7 (3.8)	7.8	31.6	26.4-36.0
Interindividual variability on Vc§ (% shrinkage)	38.3 (13.5)	21.9	39.8	24.4-56.1
Interindividual variability on Kin§ (% shrinkage)	81.9 (29.7)	10.8	81.1	60.0-97.6
f-ara-A residual unexplained variability§ (% shrinkage)	24.8 (10.7)	7.6	24.1	21.3-27.6
f-ara-ATP residual unexplained variability§ (% shrinkage)	71.5 (11.2)	9.5	71.1	63.2-78.8
Correlation	CL - Vc	.86	12.8	
	CL - Kin	.29	25.9	
	Vc -Kin	.59	20.9	

RSE indicates relative standard error; Vc volume of the central compartment; Vp, volume of the peripheral compartment.

* Relative standard error expressed as % mean.

† First-order rate constant for drug moving from the central compartment to the intracellular compartment.

‡ First-order rate constant for drug moving out of the intracellular compartment.

§ Presented as %CV.

Table 3

Observed Peak and Trough Concentrations of f-ara-ATP with Each Dose of Fludarabine

	Concentration of f-ara-ATP*					
Sample Collection Time	**Dose 1**	**Dose 2**	**Dose 3**	**Dose 4**	**Dose 5**	***P* Value†**
2 Hr after start of infusion	7.9 (.7-18)	1.5 (.5-19.8)	3.4 (.4-12)	1.7 (.2-7)	.6 (.2-1.4)	<.001
No. of samples	27	4	22	28	5	
24 Hr after start of infusion	2.0 (0-6.9)	.5 (.1-7.3)	1.0 (.3-8.3)	.9 (.1-10.3)	.5 (.1-7.2)	.57
No. of samples	33	12	25	31	6	

*Data are presented as median (range) and expressed as pmoles/million clls.

†The *P* value is based on a simple linear regression using dosing event as predictors on f-ara-ATP concentrations.

Table 4

Comparison of Daily Exposure of f-ara-a (AUC_{0-24}) in the Observed Data Presented by Fludarabine Daily Regimen

Fludarabine Regimen	n	AUC_{0-24}, median (range), mg*hour/L
All dose regimens	133	3.7 (3.3-4.5)
40 mg/m^2/dose	55	4.5 (3.7-4.8)
mg/kg/dose *	38	3.4 (3.1-3.9)

* Patients assigned to a regimen of 40 mg/m^2/day but had empiric dose reductions and dosing based on a mg/kg basis. Daily doses range from . 9-1.33 mg/kg/dose.